

SIMULATION OF IMPURITY DIFFUSION IN A  
POLYCRYSTALLINE THIN FILM

J. P. Lavine

Research Laboratories, Eastman Kodak Company,  
Rochester, New York, U.S.A. 14650

Summary

Polycrystalline thin films play a crucial role in semiconductor device fabrication, device operation, and device reliability. Thin films may serve as diffusion sources, as gates and electrodes, and as part of layered contact structures. The successful application of thin films in these settings requires an understanding of impurity diffusion in polycrystalline thin films. While the qualitative results of diffusion experiments may often be easily understood, the exploitation of the results usually demands quantitative models. If simulations are to help explain the diffusion process in thin films, they must include both grain-boundary and grain diffusion. Current models assume the grains are columnar with the grain thickness equal to the thin-film thickness, but many thin films have a multilayer grain structure.

The Monte Carlo or random-walk-on-a-lattice approach to grain-boundary diffusion originated with Brandt. This approach is extended in the present work to multiple layers of grains and to random grain patterns. Grain-boundary segregation is treated by a relative jump-time method, which is related to the transport-equation approach of Benoist and Martin. A series of examples shows how the impurity profiles depend on the diffusion coefficients and segregation parameterization. The impurity profiles for films with more than one layer of grains show secondary peaks around the depths where the horizontal grain boundaries are. This effect reduces the number of impurity particles that diffuse to the backside of the film and may play a role in diffusion barriers.

## 1. INTRODUCTION

Polycrystalline thin films play a crucial role in semiconductor device fabrication, device operation, and device reliability [1]. Thin films may serve as a diffusion source for doping those parts of the substrate where active devices are built [2-6]. Metallic thin films or doped polycrystalline silicon thin films are the gates and electrodes of the devices. Contacts are needed between the metal levels and the substrate and between the metal levels and the polysilicon or silicide electrodes. Many contact schemes involve layered structures of thin films [7-9]. The successful application of thin films in any of these settings depends on the understanding of impurity diffusion in polycrystalline thin films. Impurities diffuse along grain boundaries and through the grains. Thus, if simulations are to help explain the diffusion process, they must include these two paths. Current models assume the grain thickness equals the thickness of the thin film [10] as in Fig. 1. Yet transmission electron microscopy [11-13] shows that many thin films have more than one grain in the vertical direction. Figure 2 illustrates this situation. Thus, it is important to find a simulation method for impurity diffusion in this more complex setting. The present paper shows that a Monte Carlo or random-walk-on-a-lattice approach fills this need.

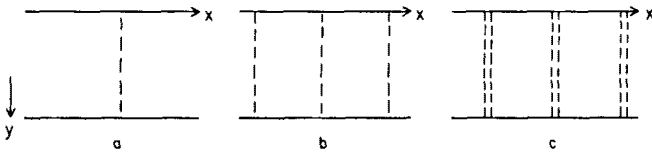


Fig. 1. Idealized thin-film cross sections for diffusion in the presence of grain boundaries (dashed lines).

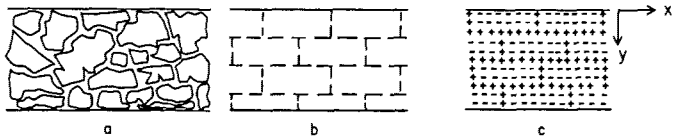


Fig. 2. More realistic thin-film cross sections with grain boundaries.

Grain-boundary diffusion is usually more rapid than diffusion through a grain, so there may be impurity diffusion at temperatures where grain diffusion is negligible. This helps to explain why semiconductor device properties may depart from expectations. Several examples serve to clarify the effects of grain-boundary impurity diffusion. Aluminum is used to contact polysilicon layers. Silicon diffuses along aluminum grain boundaries during the sintering step, which is a 400 to 500°C anneal. The diffusing silicon forms a silicon layer which increases the contact resistance to the aluminum layer [14, 15]. Silicides are now used to lower the resistance of polysilicon electrodes. In many cases the silicide is deposited or formed on top of a doped polysilicon layer. The dopant in the polysilicon may enter the silicide and change its properties [16-18]. Another illustration of grain-boundary diffusion involves the oxidation of some silicides. Here the formation of an oxide, which serves as an insulating layer, depends on silicon diffusing through the silicide layer to react with the oxygen [19]. Multilayer contact schemes are used in many devices. Generally one of the layers serves as a diffusion barrier to prevent unwanted chemical reactions or to prevent shorting [7, 8, 20-22]. Impurity diffusion in polycrystalline silicon is under active study since polysilicon is used for the electrodes in devices [2, 4, 23-26] and for the substrate in solar cells [27-29].

This paper contains an account of the Monte Carlo approach to impurity diffusion in a polycrystalline thin film. This approach, which originated with the work of Brandt [30] in 1973, is described in Section 2. The section starts with a brief review of the numerical methods used to simulate grain-boundary diffusion. Section 3 presents several applications of the Monte Carlo approach to grain-boundary diffusion. Section 4 contains conclusions.

## 2. SIMULATION OF GRAIN-BOUNDARY DIFFUSION

This section starts with a brief review of how grain-boundary-diffusion experiments are usually analyzed. This is followed by a description of the Monte Carlo approach, which involves a particle jumping on lattice sites. An impurity particle usually remains in a grain boundary for some time after its entry, owing to energy considerations. This segregation effect is not easy to simulate [30] with a Monte Carlo approach that follows one diffusing particle at a time. One simulation approach involves jump times for the various possible transitions and is related to the formulation of grain-boundary diffusion due to Benoist and Martin [31-32]. Examples show how the parameters that describe segregation affect the impurity profiles. In addition, the examples are for varied numbers of vertical grains and for a series of ratios of grain-boundary to grain diffusion coefficients.

## 2.1 Grain-boundary diffusion analysis

Impurity-diffusion experiments in polycrystalline thin films are usually analyzed with closed-form solutions to the two-dimensional diffusion equation,

$$\frac{\partial C}{\partial t} = D \left( \frac{\partial^2 C}{\partial x^2} + \frac{\partial^2 C}{\partial y^2} \right) \quad (1)$$

Here the impurity concentration is  $C$  and the impurity diffusion coefficient is  $D$ . These solutions are for the idealized geometries of Figs. 1a and 1b and they were recently reviewed by Gupta, Campbell, and Ho [10]. These approaches involve replacing the diffusion equation for the grain-boundary region by an effective boundary condition. The case of a finite-width grain, as in Fig. 1b, has also been treated numerically [33-35]. When the grain boundary is given a finite width as in Fig. 1c, then two two-dimensional diffusion equations result. These are coupled by boundary conditions at the grain boundary/grain interface [25]. In addition, solutions are available for the case where the diffusion within a grain can be neglected [36-37].

A more realistic geometry is represented by Fig. 2a [11-13]. The above approaches are not easily extended to this case, although estimates have been made of the time required to fill a grain via grain-boundary diffusion [38-40]. Barrer and Petropoulos [41] derived the steady-state flux and an effective diffusion constant for an idealized array of rectangular grains. This suggests that it is useful to study an idealization such as Fig. 2b in an attempt to describe impurity diffusion in thin films with more than one layer of grains. Numerical methods are difficult to program for the multilayer case because the equations which describe the boundary conditions are distinct from the equations which describe diffusion within a grain or a grain-boundary region. Thus, a great deal of programming is required so that grain sizes and the number of grains may be easily changed. A more flexible alternative, which is easy to program, is provided by the Monte Carlo approach.

## 2.2 Monte Carlo approach to grain-boundary diffusion

Brandt first applied the Monte Carlo method to grain-boundary diffusion problems with the geometry of Fig. 1c [30]. This approach is applied here to more general structures. The two-dimensional diffusion equation, eq. (1), is replaced by particles undergoing a random walk on a lattice. Figure 2b is now replaced by Fig. 2c, which is a lattice-site representation of a thin film with four layers of grains. The lattice sites are separated by the distance  $r$ . Each lattice site in

the grain is represented by a minus sign, and the grain boundaries appear as plus signs. The topmost layer, which starts at  $y = 0$ , has two complete grains, while the next layer has a half grain, a whole grain, and then another half grain. This pattern is repeated until the bottom of the thin film is reached. Figures 2b and 2c represent a brick-wall pattern of grains.

The boundary conditions at the top surface ( $y = 0$ ) and at the bottom surface are individually set to be either reflecting or absorbing. The top and bottom surfaces are considered to be grain boundaries. This allows a particle to diffuse horizontally when the surface is reflecting. Periodic boundary conditions are assumed on the vertical boundaries. Thus, a particle on the right edge that jumps to the right actually moves to the extreme left edge. The examples in this paper all involve particles which start at a fixed  $y$  value. The initial  $x$  coordinate is a random number uniformly distributed over the width of the model space, which is twice the width of a grain. The initial  $x$  coordinate,  $x_1$ , is then converted to the initial lattice point by finding the largest integer in  $x_1 + 1$ .

The relative jump-time approach is used to describe the particle's random walk on the lattice. This approach is analogous to the use of reaction cross sections to determine the type of scattering event a particle undergoes in Monte Carlo simulations of energy loss processes [42]. The method also parallels the transport-equation approach of Benoist and Martin to grain-boundary diffusion [31]. Each lattice site has an integer or a material index associated with it; for example, a grain site is 1 and a grain-boundary site is 2. A matrix of jump times can be defined with elements  $\tau(n,m)$ . Here  $n$  is the material index of the lattice site associated with the particle's present position, and  $m$  is the material index of a lattice site the particle may reach in one jump. These jump times represent the inverse of the probability for a particular jump to occur. The jump times for  $n = m$  are related to diffusion coefficients. The time  $\tau$  associated with such a jump is the inverse of the jump frequency  $\Gamma$ , which is related to the diffusion coefficient  $D$  by [43]

$$\Gamma = 6D/r^2 \quad (2)$$

so

$$\tau = 1/\Gamma \quad (3)$$

A jump frequency, and hence a jump time, is generated for the grain-boundary diffusion coefficient  $D_{GB}$  and for the grain diffusion coefficient  $D_G$ . The jump times for going from one material to another are parameters.

Suppose a particle is at lattice site  $(i,j)$ . Then it

may jump to sites  $(i+1,j)$ ,  $(i,j-1)$ ,  $(i-1,j)$ , or  $(i,j+1)$ , and each of these sites has its material index. Thus, four jump times can be extracted from the  $\tau(n,m)$  matrix, and these may, for illustration, be denoted as  $\tau_r$ ,  $\tau_d$ ,  $\tau_\ell$ , and  $\tau_u$ , respectively. Of course, whether any two or more of these are equal depends on where the particle is and what the material indices of the nearest-neighbor lattice sites are. Now let

$$P_T = (1/\tau_r) + (1/\tau_d) + (1/\tau_\ell) + (1/\tau_u), \quad (4)$$

and define four boundaries,

$$P_1 = (1/\tau_r)/P_T, \quad (5)$$

$$P_2 = \{(1/\tau_r) + (1/\tau_d)\}/P_T, \quad (6)$$

$$P_3 = \{(1/\tau_r) + (1/\tau_d) + (1/\tau_\ell)\}/P_T, \quad (7)$$

and

$$P_4 = 1. \quad (8)$$

The jump direction of the particle is selected by comparing a random number  $q$ , which is uniformly distributed over 0 to 1, with the  $P_i$ . For example, if  $q$  is less than  $P_3$  and greater than or equal to  $P_2$ , then the particle jumps to the left, i.e., the particle goes from site  $(i,j)$  to site  $(i-1,j)$ .

This approach treats the various types of jumps within the same formalism, which also handles segregation. The jump times for jumps into and out of a grain boundary are presently free parameters. The former is denoted by  $\tau_{G-GB}$  and the latter by  $\tau$  in the following figures. In general,  $\tau = \tau_{G-GB} = \tau_G$ , where  $\tau_G$  is related to  $D_G$  by eqs. (2) and (3). Exceptions to this are noted. The time associated with a jump is

$$\Delta t = -\tau_a \ln(1 - q') \quad (9)$$

where the  $a$  is the selected jump direction and  $q'$  is a random number uniformly distributed over 0 to 1. This method of assigning  $\Delta t$  leads to a variable time between jumps, which is appropriate for simulating diffusion.

The appropriate  $\Delta t$  is added to the particle's elapsed time, and the process is repeated. The particle performs a random walk until its elapsed time equals or exceeds the diffusion time or the particle reaches an absorbing boundary. The final coordinates of the particle are saved. Another particle is then started, and the process is repeated. After

a preset number of particles have diffused, an impurity profile is calculated by summing over all the particles with the same final  $y$  value. Then the results for four successive  $y$  values are added to provide the impurity profile displayed in the following figures.

An extensive set of results from the relative jump-time approach is now presented. The thin-film thickness is  $0.35 \mu\text{m}$ , the grain width is  $0.08 \mu\text{m}$ , the lattice-site spacing  $r_1$  is  $0.0025 \mu\text{m}$ , the diffusion time is  $960 \text{ s}$ , and  $D_G$  is  $10^{-15} \text{ cm}^2/\text{s}$ . The initial  $y$  value is  $0.06 \mu\text{m}$  to simulate an ion implant. Ten thousand particles are followed for each set of parameters, and the top and bottom surfaces are reflecting. Figures 3 and 4 are tests to see if the computer program has any bias. In both figures the filled-circle profiles are for impurities that start at  $y = 0.06 \mu\text{m}$ , and the open-circle profiles are for impurities that start at  $0.29 \mu\text{m}$ . The latter profiles have been reflected for the comparison, and no biases are evident.

The profile in Fig. 4 rises for  $y$  beyond  $0.3 \mu\text{m}$ . This is due to horizontal diffusion along the grain boundary at  $y = 0.35 \mu\text{m}$  and is also observed in the calculations of Gilmer and Farrell [35]. A new feature appears in the profile for two layers of grains. The profile has a secondary peak around the depth where there is a horizontal grain boundary, which appears to detour the particles from their downward diffusion. Secondary peaks are seen in the other examples described in this section and the next and seem to be a general feature of impurity diffusion in a multilayer thin film. Figure 5 shows the impurity profiles for a one-grain-thick film and for various ratios of  $D_{GB}/D_G$ . The profile tails are due to grain-boundary diffusion, and the magnitude of the tail increases with an increase in the grain-boundary diffusion coefficient  $D_{GB}$ . Figure 6 presents the impurity profiles for a thin film that is two grains thick. The secondary peak halfway through the film is again evident, as is the pile-up near  $y = 0.35 \mu\text{m}$ .

The relative jump-time approach simply parameterizes the times for jumps into or out of a grain boundary. The next series of figures illustrates how the impurity profiles change with  $\tau$  and  $\tau_{G-GB}$ . Figures 7 and 8 are for a one-grain-thick film. Figure 7 shows how a decrease in the jump time  $\tau$  for a jump from grain boundary to grain decreases the impurity profile tail. This decrease in  $\tau$  means it is more likely for a particle to leave a grain boundary. Figure 8 shows how a decrease in the jump time  $\tau_{G-GB}$  for a jump from grain to grain boundary increases the profile tail. This decrease means it is more likely a particle will re-enter a grain boundary once it has jumped out. Figure 9 presents results for thin films with two layers of grains and for  $D_{GB}/D_G = 10^3$ . Figure 9 has

Fig. 3. Number of particles versus depth for a film with one grain 0.35  $\mu\text{m}$  thick.  $D_{\text{GB}}/D_{\text{G}}$  is  $10^3$ , and the results are shown for each value of  $\gamma$ . Further details are in the text.

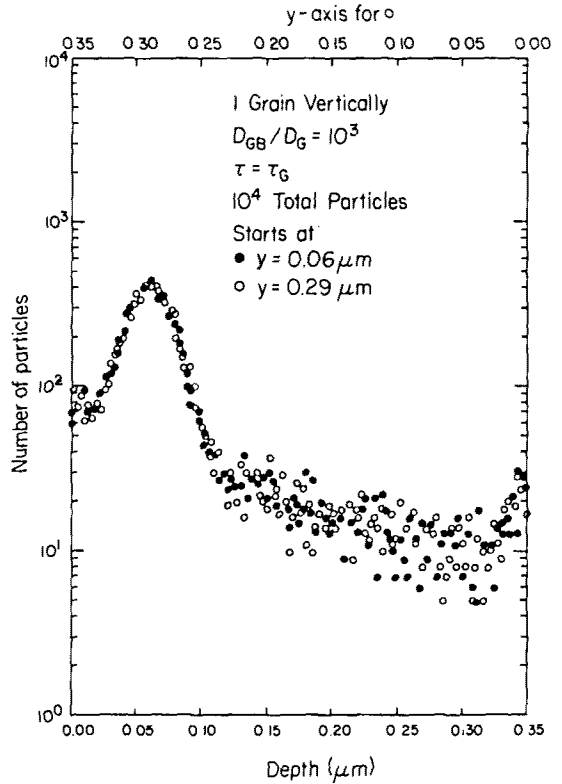


Fig. 4. Number of particles versus depth for a film with two grains vertically and a total thickness of 0.35  $\mu\text{m}$ .  $D_{\text{GB}}/D_{\text{G}}$  is  $10^3$ . Further details are in the text.

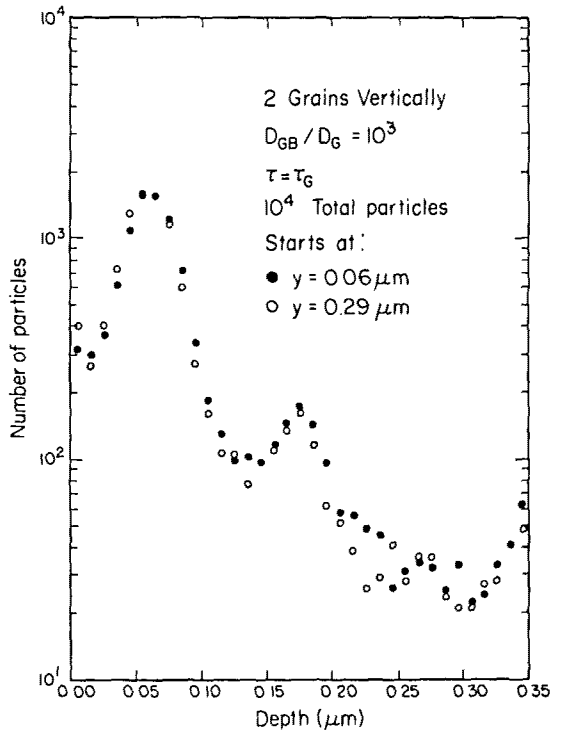




Fig. 5. Number of particles versus depth for a film with one grain  $0.35 \mu\text{m}$  thick.  $D_{\text{GB}}/D_{\text{G}}$  is varied from  $10^3$  by 10.

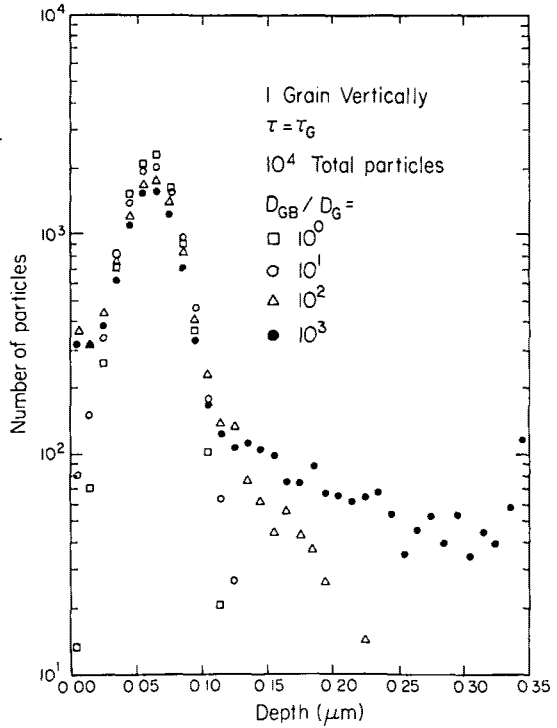


Fig. 6. Number of particles versus depth for a film with two grains vertically and a total thickness of  $0.35 \mu\text{m}$ .  $D_{\text{GB}}/D_{\text{G}}$  is  $10^2$  and  $10^3$ .

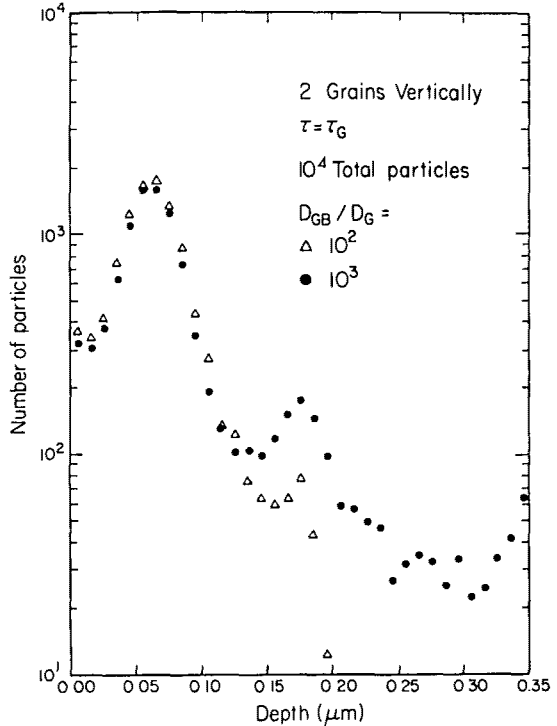


Fig. 7. Number of particles versus depth for a film with one grain  $0.35 \mu\text{m}$  thick.

$D_{\text{GB}}/D_{\text{G}}$  is  $10^3$  and  $\tau$  is  $\tau_{\text{G}}$  (filled circles) and  $\tau_{\text{G}}/10$  (open triangles).

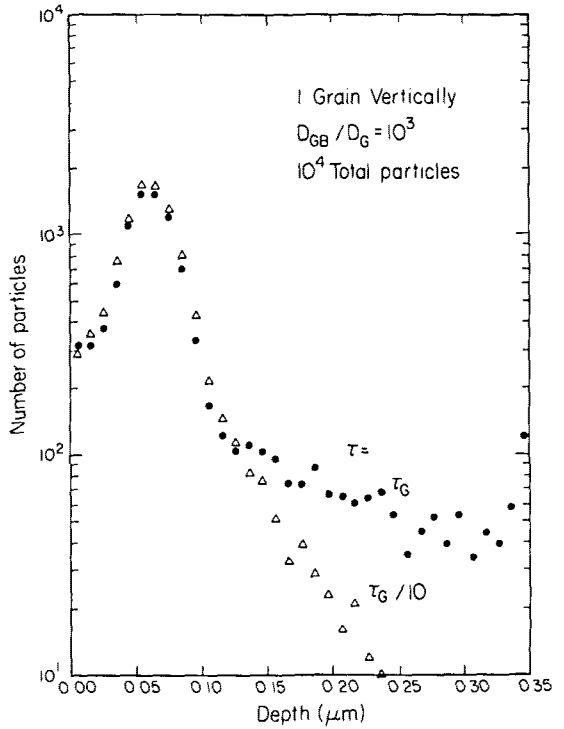
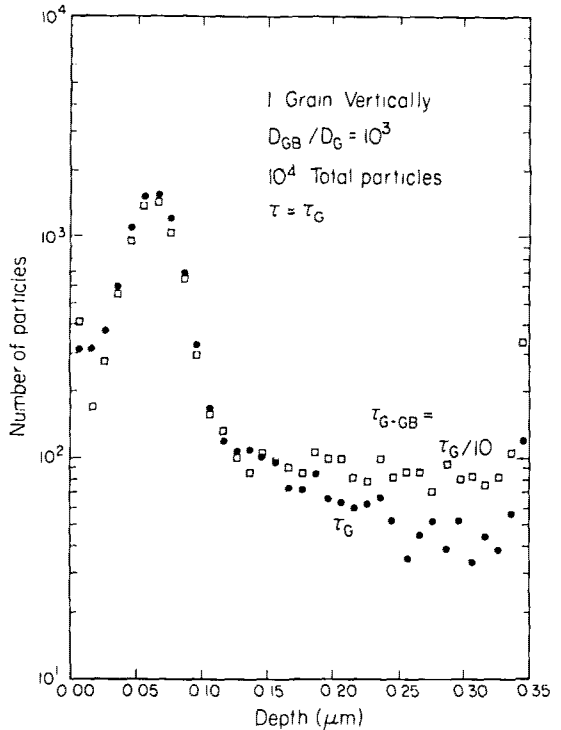


Fig. 8. Number of particles versus depth for a film with one grain  $0.35 \mu\text{m}$  thick.

$D_{\text{GB}}/D_{\text{G}}$  is  $10^3$ ,  $\tau$  is  $\tau_{\text{G}}$ , and  $\tau_{\text{G-GB}}$  is  $\tau_{\text{G}}$  (filled circles) and  $\tau_{\text{G}}/10$  (open squares).



the filled circles as the standard case with  $\tau = \tau_{G-GB} = \tau_G$ . The open triangles show how the profile tail is sharply decreased when  $\tau$  is reduced by a factor of 10. The open circles have  $\tau = \tau_G$ , but now  $\tau_{G-GB}$  is reduced by a factor of 3 and the secondary peak is increased. Once again, these results may be understood in terms of a particle staying in a grain boundary or re-entering one.

### 3. APPLICATIONS

This section contains several applications of the relative jump-time formulation of the Monte Carlo approach to grain-boundary diffusion. More examples will be presented at the International Conference on Simulation of Semiconductor Devices and Processes.

The first example uses the parameters of the Section 2 examples with a two-grain-thick film,  $D_{GB}/D_G = 10^3$ , and  $\tau = \tau_G = \tau_{G-GB}$ . Figure 10 shows how the impurity profile tail increases in magnitude when the grain width is reduced from 0.08 to 0.02  $\mu\text{m}$ . The last case is so narrow that most of the particles encounter a grain boundary, which causes the main peak to be significantly reduced in comparison to the other cases. The secondary peak is also reduced when the grain narrows. The particles diffusing horizontally along the grain boundary cross a vertical grain boundary sooner in a narrower grain. The results of Fig. 10 conform to general expectations about grain-boundary diffusion, i.e., there is increased diffusion when the grain width is decreased [8, 15].

The second example is also concerned with how grain-boundary diffusion is affected by narrower grains, but now the thickness of the grains is also varied. This example is inspired by the experiments of Hwang et al. [26], by the contact problem of Lo and co-workers [21, 22] and by the studies of problems with aluminum metallization [8, 15]. The thin-film thickness is 0.35  $\mu\text{m}$ , the lattice-site spacing is 0.0025  $\mu\text{m}$ , the diffusion coefficient within a grain  $D_G$  is  $10^{-17} \text{ cm}^2/\text{s}$ , and the ratio  $D_{GB}/D_G$  is  $10^5$ . The  $D_G$  value means that diffusion within a grain is negligible. The value of  $\tau$  is  $\tau_G/10$ , and  $\tau_{G-GB}$  is also  $\tau_G/10$ . The impurity particles are started at  $y = 0$ , which is a grain boundary and a reflecting surface. The backside of the thin film at  $y = 0.35 \mu\text{m}$  is an absorbing surface. The above conditions simulate the experiments referred to above, which deal with situations with only grain-boundary diffusion.

Figure 11 shows how many particles are absorbed by the backside as a function of the diffusion time. One thousand

Fig. 9. Number of particles versus depth for a film with two grains vertically and a total thickness of  $0.35 \mu\text{m}$ .  $D_{\text{GB}}/D_{\text{G}}$  is  $10^3$ . Further details are in the text.

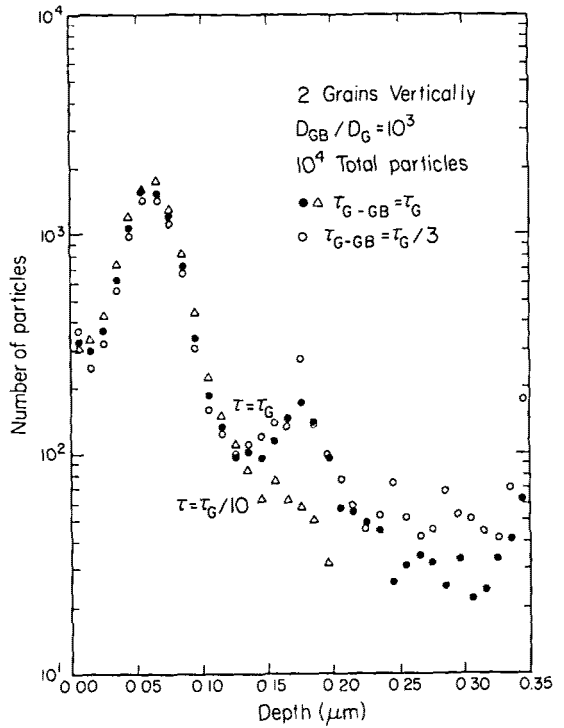
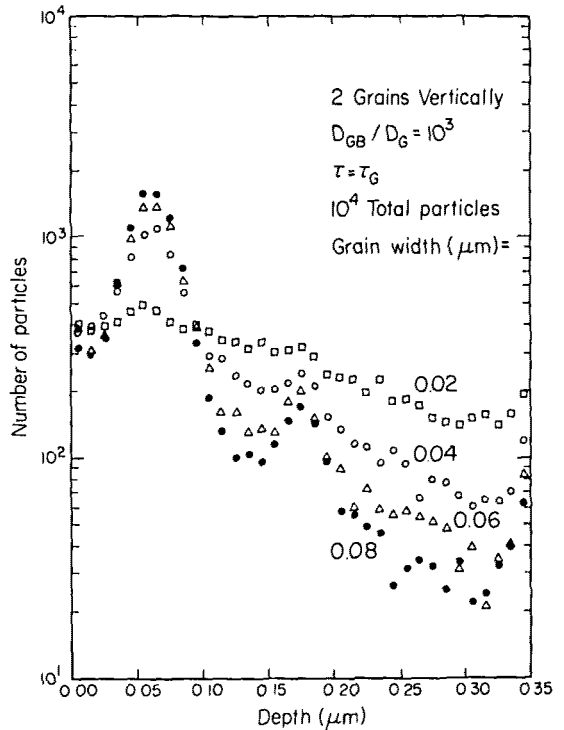


Fig. 10. Number of particles versus depth for a film with two grains and a total thickness of  $0.35 \mu\text{m}$ .  $D_{\text{GB}}/D_{\text{G}}$  is  $10^3$ ,  $\tau$  is  $\tau_{\text{G}}$ , and  $\tau_{\text{G-GB}}$  is  $\tau_{\text{G}}$ . The grain width is  $0.08 \mu\text{m}$  (filled circles),  $0.06 \mu\text{m}$  (open triangles),  $0.04 \mu\text{m}$  (open circles), and  $0.02 \mu\text{m}$  (open squares).



particles are followed for each case, and the grain width is  $0.04 \mu\text{m}$ . For a fixed diffusion time fewer particles reach the backside when the number of grains in the vertical direction is increased. The results are for thin films with one (filled circles), two (filled triangles), and ten (filled squares) grains vertically. The remaining particles are located along grain boundaries, and there are more of these to detour the particles in the multilayer films. The curves of Fig. 11 show the general shape expected by the solutions of Hwang and Balluffi [36] for a one-grain-thick film, although the dependence on the time  $t$  is more complicated than a single exponential with a parameter  $s$ ,

$$1.0 - e^{-st} \quad (10)$$

The results show an approximate linear dependence on time only at short times. This contrasts with the experimental results of Hwang et al. [26], although the error bars of their Fig. 5 may encompass a shape like that of eq. (10). A rough evaluation of  $s$  for their experiment, which is done with the aid of Section III B of Ref. 36, suggests that  $s$  is not small.

Figure 12 presents further results for this example. The diffusion time is now fixed at 900 s, and the grain width is  $0.04 \mu\text{m}$  (filled circles) or  $0.08 \mu\text{m}$  (open circles). The number of particles absorbed at the backside is shown as a function of the number of layers of grains. The number of layers or the number of vertical grains varies from 1 to 35. In all cases the total thin-film thickness is fixed at  $0.35 \mu\text{m}$ . Figure 12 shows that the horizontal grain boundaries are quite effective in reducing the flux of particles to the backside. Thus, it appears that finer grains vertically lead to less and not more diffusion.

The final application involves a more general grain pattern than the brick-wall pattern. The thin-film thickness is  $0.07 \mu\text{m}$ , the lattice-site spacing is  $0.0005 \mu\text{m}$ , the grain width is  $0.035 \mu\text{m}$ , the diffusion time is 900 s, the diffusion coefficient in the grain  $D_G$  is  $10^{-16} \text{cm}^2/\text{s}$ , the ratio  $D_{GB}/D_G$  is  $10^3$ , and  $\tau = \tau_G = \tau_{G-GB}$ . The top and bottom surfaces are reflecting, and the impurity particles start at  $y = 0.015 \mu\text{m}$ . Figure 13 shows the impurity profiles for films with 1, 2, and 4 grains vertically. The profile features are the same as those presented in Section 2 and appear here for comparison with Fig. 14, which has results for computer-generated random grain patterns. For Fig. 14 the model space is  $0.25 \mu\text{m}$  wide so that the periodic boundary condition on the vertical edges does not play a large role in the diffusion. There are 9 and 18 grains for profiles a (filled circles) and b (open circles), respectively. The actual grain-boundary patterns appear in Figs. 15 and 16. The impurity profiles do not show the second-

Fig. 11. Number of particles absorbed at the backside of a 0.35- $\mu\text{m}$ -thick film versus the diffusion time.  $D_{GB}/D_G$  is  $10^5$ , the grain width is 0.04  $\mu\text{m}$ , and  $\tau = \tau_{G-GB} = \tau_G/10$ . Further details are in the text.

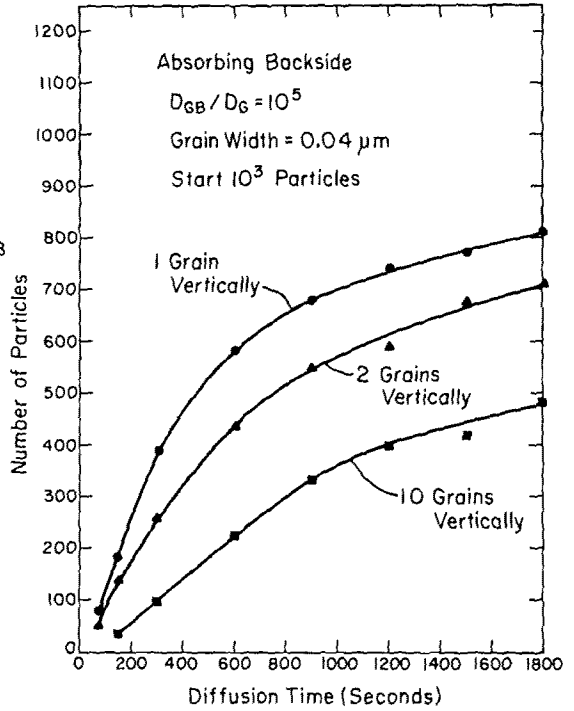


Fig. 12. Number of particles absorbed at the backside of a 0.35- $\mu\text{m}$ -thick film versus the number of vertical grains, which is the number of layers of grains.  $D_{GB}/D_G$  is  $10^5$ ,  $\tau = \tau_{G-GB} = \tau_G/10$ , and the grain width is 0.08  $\mu\text{m}$  (open circles) and 0.04  $\mu\text{m}$  (filled circles)

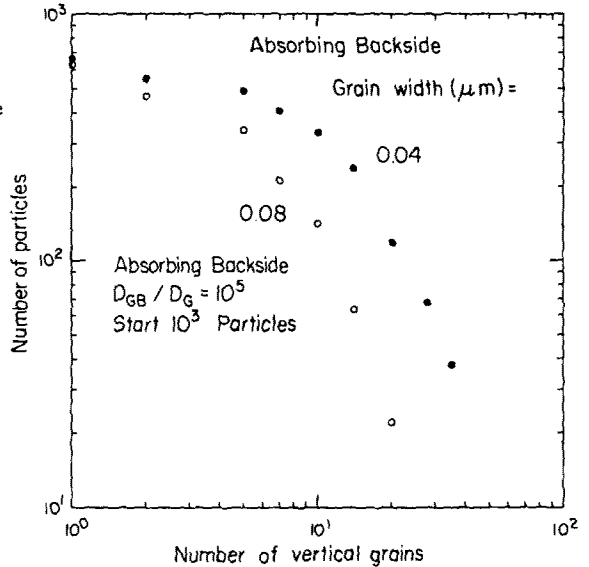


Fig. 13. Number of particles versus depth for a film  $0.07 \mu\text{m}$  thick.  $D_{GB}/D_G$  is  $10^3$ ,  $\tau = \tau_G = \tau_{G-GB}$ , the grain width is  $0.035 \mu\text{m}$ , and the particles start at  $y = 0.015 \mu\text{m}$ . There are 1, 2, and 4 grains vertically.

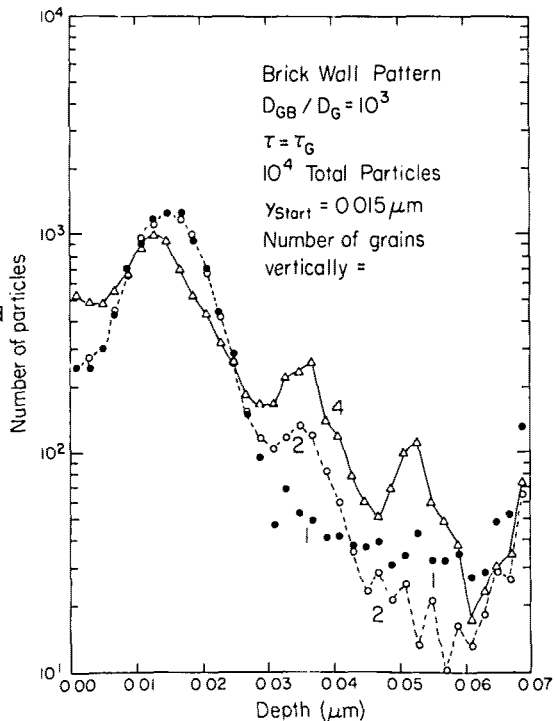
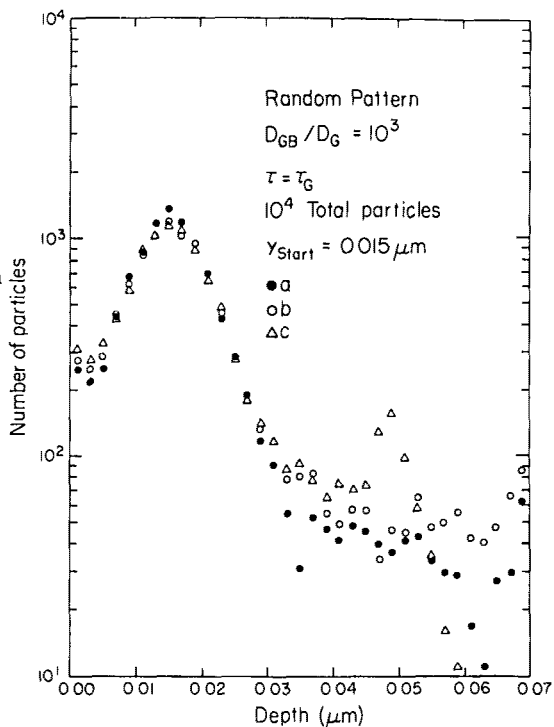


Fig. 14. Number of particles versus depth for a film  $0.07 \mu\text{m}$  thick.  $D_{GB}/D_G$  is  $10^3$ ,  $\tau = \tau_G = \tau_{G-GB}$ , and the particles start at  $y = 0.015 \mu\text{m}$ . The grain pattern is random, and the three profiles are discussed in the text.



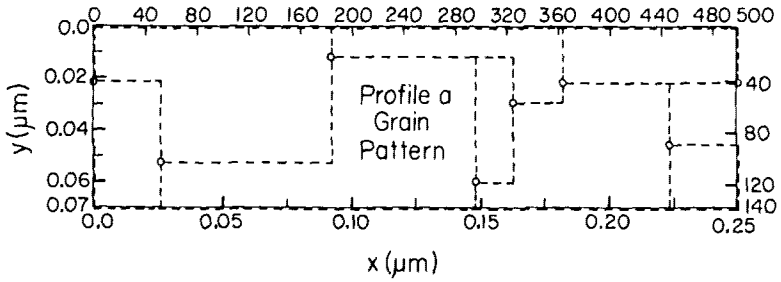


Fig. 15. The grain-boundary pattern for case a of Fig. 14.

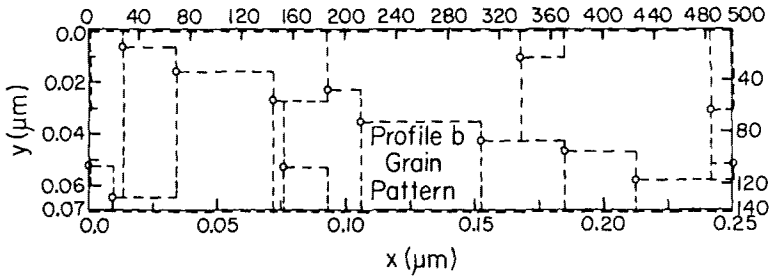


Fig. 16. The grain-boundary pattern for case b of Fig. 14.

ary peaks of Fig. 13. A generalization of the basic computer program leads to profile c (open triangles) of Fig. 14. After the grain-boundary pattern of Fig. 16 is generated, all the grain-boundary lattice sites at  $y > 0.049 \mu\text{m}$  are converted to grain sites. This permits the modeling of impurity diffusion from a polysilicon source into a crystalline silicon substrate [2-6]. Profile c shows a sharp decrease into the substrate, which is due to the small value of  $D_G$  with respect to  $D_{GB}$ . A pile-up of impurities is observed just before  $y = 0.049 \mu\text{m}$ , and this is due to the termination of the grain boundaries and to the reduced diffusion coefficient for diffusion through the grain. This pile-up has been observed [4, 44].

#### 4. CONCLUSIONS

The last two sections have presented a Monte Carlo approach to simultaneous grain-boundary and grain impurity diffusion in thin films. The introduction and Section 3 demonstrate the wide variety of semiconductor device problems in which impurity diffusion plays a role. The Monte Carlo method is easy to program and can treat a wide range of diffusion problems. It is not restricted to films with a thickness of only one grain nor to cases where grain-boundary diffusion dominates.



The major disadvantage of the Monte Carlo method is the large amount of computer time required. Most of the cases in this paper required ~30 min on an IBM model 3033 computer. It appears that the computer time increases linearly with any parameter that is likely to increase the number of jumps. The bulk of the time is spent generating random numbers. This time requirement presently precludes three-dimensional simulations of grain-boundary diffusion, although Brandt [30] reports some results in this area. The need for three spatial dimensions increases as the grain sizes get finer and the grain patterns become more random.

A conclusion may be drawn from the Monte Carlo results themselves. The presence of horizontal grain boundaries leads to secondary peaks in the impurity profile when the grain pattern resembles a brick wall [45]. It may be possible to see these peaks experimentally. If a profiling method such as secondary-ion mass spectroscopy, Rutherford backscattering, or Auger electron spectroscopy is used, then the impurity profile versus depth is available and the peaks may be seen. It would be necessary to make sure the impurity has not formed a precipitate, which appears to be the case in the experiments of Hwang et al. [26]. In fact, the secondary peaks may explain how an impurity concentration can appear to exceed solid solubility without precipitation. In addition, the finer-grain studies of Section 3 show that the horizontal grain boundaries reduce the number of impurity particles that diffuse to the backside. This result should be of use in designing and evaluating diffusion barriers [7].

In summary, a Monte Carlo method has been applied to simultaneous grain-boundary and grain impurity diffusion. Calculations have been carried out for a variety of single-grain and multigrain thin films. Further applications of the model to experimental situations in the literature are planned.

#### Acknowledgements

I thank R. A. Phillips for his generous help in using a complicated computer system. Helpful conversations with B. C. Burkey, S.-T. Lee, D. L. Losee, E. T. Nelson, and E. A. Trabka are gratefully acknowledged.

#### REFERENCES

1. POATE, J. M., TU, K. N. and MAYER, J. W.  
Thin Films - Interdiffusion and Reactions  
Wiley, New York, 1978.
2. TSUKAMOTO, K., AKASAKA, Y. and HORIE, K.  
"Arsenic Implantation Into Polycrystalline Silicon  
and Diffusion to Silicon Substrate"  
J. Appl. Phys, Vol. 48, p. 1815, 1977.

3. OKADA, K., AOMURA, K., NAKAMURA, T. and SHIBA, H.  
"A New Polysilicon Process for a Bipolar Device - PSA Technology"  
IEEE Trans. Electron Dev. Vol. ED-26, p. 385, 1979.
4. RYSSEL, H., et al.  
"Arsenic-Implanted Polysilicon Layers"  
Appl. Phys. Vol. 24, p. 197, 1981.
5. BARSON, F., KASTL, R., KEMLAGE, B. and MICHEL, A.  
"Shallow Bipolar Transistor Profiles by Diffusion from Implanted Polysilicon", In: VLSI Science and Technology/1982 (Ed. C. J. Dell'Oca and W. M. Bullis), The Electrochemical Society, Pennington, N.J., p. 282, 1982.
6. JOSQUIN, W.J.M.J., BOUDEWIJN, P. R. and TAMMINGA, Y.  
"Effectiveness of Polycrystalline Silicon Diffusion Sources"  
Appl. Phys. Lett. Vol. 43, p. 960, 1983.
7. NICOLET, M.-A. and BARTUR, M.  
"Diffusion Barriers in Layered Contact Structures"  
J. Vac. Sci. Technol. Vol. 19, p. 786, 1981.
8. KRUSIN-ELBAUM, L., WITTMER, M., TING, C.-Y. and CUOMO, J. J.  
"ZrN Diffusion Barrier in Aluminum Metallization Schemes"  
Thin Solid Films Vol. 104, p. 81, 1983.
9. SCOTT, D.M., et al.  
"The Effects of Interfacial SiO<sub>2</sub> on Pd<sub>2</sub>Si Formation"  
Thin Solid Films Vol. 104, p. 227, 1983.
10. GUPTA, D., CAMPBELL, D. R. and HO, P.S.  
"Grain Boundary Diffusion", In: Thin Films- Interdiffusion and Reactions (Ed. J. M. Poate, et al.), Wiley, New York, p. 161, 1978.
11. OPPOLZER, H., FALCKENBERG, R. and DOERING, E.  
"Cross-sectional Transmission Electron Microscopy for Polycrystalline Silicon Films"  
J. Microsc. Vol. 118, p. 97, 1980.
12. OPPOLZER, H. and HUBER, V.  
"Details of Microstructure and Geometrical Configuration of Integrated Circuits Studied by Transmission Electron Microscopy", In: Microscopy of Semiconducting Materials, 1983 (Ed. A. G. Cullis, et al.), The Institute of Physics, Bristol and London, p. 461, 1983.
13. DUFFY, M. T., et al.  
"LPCVD Polycrystalline Silicon: Growth and Physical Properties of Diffusion-Doped, Ion-Implanted, and Undoped Films"  
RCA Rev. Vol. 44, p. 313, 1983.
14. LEARN, A. J. and NOWICKI, R. S.  
"Methods for Minimizing Silicon Regrowth in Aluminum Films"  
Appl. Phys. Lett. Vol. 35, p. 611, 1979.

15. NOWICKI, R. S. and LEARN, A. J.  
"Studies of Silicon Regrowth with Aluminum and Aluminum Alloy Metallizations"  
Thin Solid Films Vol. 67, p. 385, 1980.
16. PELLEG, J. and MURARKA, S. P.  
"Phosphorus Distribution in TaSi<sub>2</sub> Films by Diffusion From a Polycrystalline Silicon Layer"  
J. Appl. Phys. Vol. 54, p. 1337, 1983.
17. TSAI, M. Y., et al.  
"One-Micron Polycide (WSi<sub>2</sub> on Poly-Si) MOSFET Technology"  
J. Electrochem. Soc. Vol. 128, p. 2207, 1981.
18. JAHNEL, F., et al.  
"The Behavior of Boron (also Arsenic) in Bilayers of Polycrystalline Silicon and Tungsten Disilicide"  
J. Appl. Phys. Vol. 53, p. 7372, 1982.
19. ZIRINSKY, S., HAMMER, W., D'HEURLE, F. and BAGLIN, J.  
"Oxidation Mechanisms in WSi<sub>2</sub> Thin Films"  
Appl. Phys. Lett. Vol. 33, p. 76, 1978.
20. DOYLE, B. L., et al.  
"Atomic Interdiffusion in Au/Amorphous Ni-Nb/  
Semiconductor Systems"  
Thin Solid Films Vol. 104, p. 69, 1983.
21. LO, W. and GIFFORD, F. E.  
"Contact Reliability Studies on Lead-Salt Diode Lasers"  
J. Electrochem. Soc. Vol. 127, p. 1372, 1980.
22. LO, W.  
"Highly Reliable Contacts for Lead-Salt Diode Lasers"  
J. Appl. Phys. Vol. 52, p. 900, 1981.
23. SWAMINATHAN, B., et al.  
"Diffusion of Arsenic in Polycrystalline Silicon"  
Appl. Phys. Lett. Vol. 40, p. 795, 1982.
24. BUONAQUISTI, A. D., CARTER, W. and HOLLOWAY, P. H.  
"Diffusion Characteristics of Boron and Phosphorus in Polycrystalline Silicon"  
Thin Solid Films Vol. 100, p. 235, 1983.
25. LOSEE, D. L., LAVINE, J. P., TRABKA, E. A., LEE, S.-T. and JARMAN, C. M.  
"Phosphorus Diffusion in Polycrystalline Silicon"  
J. Appl. Phys. Vol. 55, p. 1218, 1984.
26. HWANG, J.C.M., et al.  
"Grain Boundary Diffusion of Aluminum in Polycrystalline Silicon Films"  
J. Appl. Phys. Vol. 51, p. 1576, 1980.
27. NEUGROSCHER, A. and MAZER, J. A.  
"Effects of Grain Boundaries on the Current-Voltage Characteristics of Polycrystalline Silicon Solar Cells"  
IEEE Trans. Electron. Dev. Vol. ED-29, p. 225, 1982.
28. JAIN, G. C., CHAKRAVARTY, B. C. and SINGH, S. N.  
"Dopant Profile Analysis of Boron in Solar Grade Poly- and Single-Crystalline Silicon"  
Appl. Phys. Lett. Vol. 38, p. 815, 1981.

29. DI STEFANO, T. H. and CUOMO, J. J.  
"Reduction of Grain Boundary Recombination in Polycrystalline Silicon Solar Cells"  
Appl. Phys. Lett. Vol. 30, p. 351, 1977.
30. BRANDT, W. W.  
"Monte Carlo Simulation of Simultaneous Bulk, Grain Boundary, and Surface Diffusion"  
J. Chem. Phys. Vol. 59, p. 5562, 1973.
31. BENOIST, P. and MARTIN, G.  
"Atomic Model for Grain Boundary and Surface Diffusion"  
Thin Solid Films Vol. 25, p. 181, 1975.
32. BENOIST, P. and MARTIN, G.  
"Modèle Atomique de Diffusion Intergranulaire: Généralisation"  
J. Phys. (Paris) Vol. C4, p. C4-213, 1975.
33. UNNAM, J., CARPENTER, J. A. and HOUSKA, C. R.  
"X-ray Diffraction Approach to Grain Boundary and Volume Diffusion"  
J. Appl. Phys. Vol. 44, p. 1957, 1973.
34. HOLLOWAY, P. H., AMOS, D. E. and NELSON, G. C.  
"Analysis of Grain-Boundary Diffusion in Thin Films: Chromium in Gold"  
J. Appl. Phys. Vol. 47, p. 3769, 1976.
35. GILMER, G. H. and FARRELL, H. H.  
"Grain-Boundary Diffusion in Thin Films. II. Multiple Grain Boundaries and Surface Diffusion"
36. HWANG, J.C.M. and BALLUFFI, R. W.  
"Measurement of Grain-Boundary Diffusion at Low Temperatures by the Surface Accumulation Method. I. Method and Analysis"  
J. Appl. Phys. Vol. 50, p. 1339, 1979.
37. HWANG, J.C.M., PAN, J. D. and BALLUFFI, R. W.  
"Measurement of Grain-Boundary Diffusion at Low Temperature by the Surface-Accumulation Method. II. Results for Gold-Silver System"  
J. Appl. Phys. Vol. 50, p. 1349, 1979.
38. ZAESCHMAR, G.  
"Theory of Diffusion in a Polycrystalline Material"  
J. Appl. Phys. Vol. 54, p. 2281, 1983.
39. OISHI, Y. and ICHIMURA, H.  
"Grain-Boundary Enhanced Interdiffusion in Polycrystalline CaO-Stabilized Zirconia System"  
J. Chem. Phys. Vol. 71, p. 5134, 1979.
40. LEVINE, H. S. and MAC CALLUM, C. J.  
"Grain Boundary and Lattice Diffusion in Polycrystalline Bodies"  
J. Appl. Phys. Vol. 31, p. 595, 1960.
41. BARRER, R. M. and PETROPOULOS, J. H.  
"Diffusion in Heterogeneous Media: Lattices of Parallelepipeds in a Continuous Phase"  
Brit. J. Appl. Phys. Vol. 12, p. 691, 1961.

42. ZERBY, C. D.  
"A Monte Carlo Calculation of the Response of Gamma-Ray Scintillation Counters", In: Methods in Computational Physics (Ed. B. Alder, S. Fernbach, and M. Rotenberg) Academic Press, New York, Vol. 1, p. 89, 1963.
43. SHEWMON, P. G.  
Diffusion in Solids  
McGraw-Hill, New York, p. 52, 1963.
44. ARIENZO, M., KOMEM, Y. and MICHEL, A.E.  
"Diffusion of Arsenic in Bilayer Polycrystalline Silicon Films"  
J. Appl. Phys. Vol. 55, p. 365, 1984.
45. LAVINE, J. P. and LOSEE, D. L.  
"A Monte Carlo Treatment of Impurity Diffusion in Polycrystalline Films"  
J. Appl. Phys. To appear.